



Rapid precipitation of amorphous silica in experimental systems with nontronite (NAu-1) and *Shewanella oneidensis* MR-1

Yoko Furukawa *, S.E. O'Reilly

Naval Research Laboratory, Seafloor Sciences Branch, Stennis Space Center, MS 39529, USA

Received 12 May 2006; accepted in revised form 11 September 2006

Abstract

Nanometer-size (<50 nm) precipitates of amorphous silica globules were observed in laboratory systems containing nontronite NAu-1, *Shewanella oneidensis* strain MR-1, and lean aqueous media. Their formation was attributed to the release of polysilicic acids at the expense of dissolving NAu-1, and subsequent polymerization and stabilization mediated by biomolecules. Rapid (<24 h) silica globule formation was confirmed in the immediate vicinity of bacterial cells and extracellular polymeric substances in all experimental systems that contained bacteria, whether the bacteria were respiring dissolved O₂ or Fe(III) originating from NAu-1, and whether the bacteria were viable or heat-killed. Silica globules were not observed in bacteria- and biomolecule-free systems. Thermodynamic calculations using disilicic acid, rather than monomeric silica, as the primary aqueous silica species suggest that the systems may have been supersaturated with respect to amorphous silica even though they appeared to be undersaturated if all aqueous silica was assumed to be monomeric H₄SiO₄. The predominant aqueous silica species in the experimental systems was likely polysilicic acids because aqueous silica was continuously supplied from the concurrent dissolution of aluminosilicate. Further polymerization and globule formation may have been driven by the presence of polyamines, a group of biologically produced compounds that are known to drive amorphous silica precipitation in diatom frustules. Globules were likely to be positively charged in our systems due to chemisorption of organic polycations onto silica surfaces that would have been otherwise negatively charged. We propose the following steps for the formation of nanometer-size silica globules in our experimental systems: (i) continuous supply of polysilicic acids due to NAu-1 dissolution; (ii) polysilicic acid polymerization to form <50 nm silica globules and subsequent stabilization mediated by microbially produced polyamines; (iii) charge reversal due to chemisorption of organic polycations; and (iv) electrostatic attraction of positively charged silica globules to net negatively charged bacterial cells. Rapid, biogenic precipitation of silica may be common in soil and sediment systems that appear to be undersaturated with respect to amorphous Si.

Published by Elsevier Inc.

1. Introduction

Precipitation of amorphous silica in the immediate vicinity of microorganism cells and associated extracellular polymeric substances (EPS) has been recognized in natural systems such as the areas surrounding seafloor hydrothermal vents, geothermal hot springs, and among volcanic glasses and ashes where interstitial waters can become locally enriched with dissolved Si and Al (Konhauser and Ferris, 1996; Asada and Tazaki, 2001; de Ronde et al.,

2002; Kawano and Tomita, 2002; Konhauser et al., 2002). Amorphous silica precipitation in association with microbial activities has been observed in laboratory systems in which aqueous phases were supersaturated with respect to amorphous silica and aluminosilicate (Toporski et al., 2002; Yee et al., 2003). In addition, amorphous silica precipitation was observed after 30 days in an experiment in which the bulk solution was slightly undersaturated with respect to amorphous silica (Kawano and Tomita, 2001). Adsorption of Si on the cell walls of *Bacillus subtilis*, cultured in silica-undersaturated media, was confirmed; the cell surface-amorphous silica association was reinforced by the presence of metal cations such as Fe³⁺ and Al³⁺ that operated as bridges between negatively charged

* Corresponding author.

E-mail address: yoko.furukawa@nrlssc.navy.mil (Y. Furukawa).

REPORT DOCUMENTATION PAGE

Form Approved
OMB No. 0704-0188

The public reporting burden for this collection of information is estimated to average 1 hour per response, including the time for reviewing instructions, searching existing data sources, gathering and maintaining the data needed, and completing and reviewing the collection of information. Send comments regarding this burden estimate or any other aspect of this collection of information, including suggestions for reducing the burden, to Department of Defense, Washington Headquarters Services, Directorate for Information Operations and Reports (0704-0188), 1215 Jefferson Davis Highway, Suite 1204, Arlington, VA 22202-4302. Respondents should be aware that notwithstanding any other provision of law, no person shall be subject to any penalty for failing to comply with a collection of information if it does not display a currently valid OMB control number.

PLEASE DO NOT RETURN YOUR FORM TO THE ABOVE ADDRESS.

1. REPORT DATE (DD-MM-YYYY) 110906		2. REPORT TYPE Journal Article		3. DATES COVERED (From - To)	
4. TITLE AND SUBTITLE Rapid precipitation of amorphous silica in experimental systems with nontronite (NAu-1) and Shewanella oneidensis MR-1				5a. CONTRACT NUMBER	
				5b. GRANT NUMBER	
				5c. PROGRAM ELEMENT NUMBER 061153N	
6. AUTHOR(S) Yoko Furukawa, S.E. O'Reilly				5d. PROJECT NUMBER	
				5e. TASK NUMBER	
				5f. WORK UNIT NUMBER	
7. PERFORMING ORGANIZATION NAME(S) AND ADDRESS(ES) Naval Research Laboratory Seafloor Sciences Branch Stennis Space Center, MS 39529				8. PERFORMING ORGANIZATION REPORT NUMBER NRL/JA/7430-04-13	
9. SPONSORING/MONITORING AGENCY NAME(S) AND ADDRESS(ES) Office of Naval Research 800 North Quincy Street Arlington VA 22217-5660				10. SPONSOR/MONITOR'S ACRONYM(S) ONR	
				11. SPONSOR/MONITOR'S REPORT NUMBER(S)	
12. DISTRIBUTION/AVAILABILITY STATEMENT Approved for public release; distribution is unlimited					
13. SUPPLEMENTARY NOTES Geochimica et Cosmochimica Acta 74 (2007) 363-377					
14. ABSTRACT Nanometer-size (<50 nm) precipitates of amorphous silica globules were observed in laboratory systems containing nontronite NAu-1, <i>Shewanella oneidensis</i> strain MR-1, and lean aqueous media. Their formation was attributed to the release of polysilicic acids at the expense of dissolving NAu-1, and subsequent polymerization and stabilization mediated by biomolecules. Rapid (<24 h) silica globule formation was confirmed in the immediate vicinity of bacterial cells and extracellular polymeric substances in all experimental systems that contained bacteria, whether the bacteria were respiring dissolved O ₂ or Fe(III) originating from NAu-1, and whether the bacteria were viable or heat-killed. Silica globules were not observed in bacteria- and biomolecule-free systems. Thermodynamic calculations using disilicic acid, rather than monomeric silica, as the primary aqueous silica species suggest that the systems may have been supersaturated with respect to amorphous silica even though they appeared to be undersaturated if all aqueous silica was assumed to be monomeric H ₄ SiO ₄ . The predominant aqueous silica species in the experimental systems was likely polysilicic acids because aqueous silica was					
15. SUBJECT TERMS					
16. SECURITY CLASSIFICATION OF:			17. LIMITATION OF ABSTRACT SAR	18. NUMBER OF PAGES 15	19a. NAME OF RESPONSIBLE PERSON Yoko Furukawa
a. REPORT Unclassified	b. ABSTRACT Unclassified	c. THIS PAGE Unclassified			19b. TELEPHONE NUMBER (include area code) 228-688-5474

cell surfaces and neutrally charged H_4SiO_4 (aq) (Urrutia and Beveridge, 1994; Fein et al., 2002; Phoenix et al., 2003). The precipitation of amorphous silica was microscopically observed on the surface of *Thiobacillus* in acidic media (Fortin and Beveridge, 1997), whereas a synchrotron Fourier-transform infrared spectroscopy study suggested that amorphous silica precipitation in supersaturated solution occurs predominantly within EPS rather than at the surface of microbial cell walls, possibly initiated by the hydrogen bonding of silica to EPS (Benning et al., 2004).

Amorphous, biogenic silica derived from diatoms is abundant in marine environments and is generally considered to be a significant participant in global silicon cycling (Ragueneau et al., 2000; Conley, 2002). Amorphous silica formation mediated by diatoms generally occurs in marine surface waters undersaturated with respect to amorphous silica (Spencer, 1983). Littoral burial of biogenic Si and formation of its immediate recrystallization product, poorly crystalline aluminosilicates, are recognized as significant processes in the global elemental budget (Michalopoulos and Aller, 2004). Moreover, microbially mediated precipitation of silica is important from the perspective of early life because much of our current understanding of early life comes from investigations of silicified microfossils or their perceived counterparts in modern hydrothermal environments (Konhauser and Ferris, 1996; Jones et al., 1997; Toporski et al., 2002). Chert layers in Precambrian banded iron formations, which have been studied extensively due to their potential role in constraining the magnitude of atmospheric O_2 concentrations on early Earth (Kasting, 1991; Ohmoto et al., 1993; Canfield, 1998), are considered to be of biogenic origin (Konhauser and Ferris, 1996).

Despite the potential importance and large number of recent studies, our understanding of the formation of amorphous silica in common soil and sedimentary environments rich in microbial activities is still limited. Field studies have focused on specific and rather unique environments such as those within volcanic ash deposits, hydrothermal vents, and geothermal springs where very high concentrations of aqueous silica are common. Many of the experiments in the literature were also conducted using aqueous solutions highly supersaturated with respect to amorphous silica and aluminosilicates (Francis et al., 1978; Westall et al., 1995; Yee et al., 2003; Benning et al., 2004). These mimic hot springs environments but do not represent interstitial waters of ordinary soils and sediments in which silica supply is likely from a gradual weathering or dissolution of silicate minerals. A few experimental studies with silica-undersaturated solution have concluded that there was minimal association between microorganism cell surfaces and silica (Fein et al., 2002; Yee et al., 2003). However, these studies focused on certain species of cyanobacteria and *Bacillus subtilis*, a gram positive bacterium, under specific laboratory conditions with lean aqueous solutions, while the interaction between microorganism cell surfaces and monomeric aqueous silica is suspected to be species- and environment-specific (Konhauser et al., 2004). In addition, most of the experimental stud-

ies of microbially mediated silica precipitation introduced above have been conducted under aerobic conditions, making their applicability to the modern and ancient sediment/soil environments somewhat constrained as the O_2 availability is in general limited or oscillating in most of these environments.

In this study, we established laboratory model systems that mimic ordinary soil and sedimentary environments in which interactions occur between a model facultative anaerobe (*Shewanella oneidensis* MR-1), model dioctahedral clay mineral (nontronite NAu-1), and aqueous interstitial water (low ionic strength, lean, and defined media). The clay mineral is the only source of Si for the formation of amorphous silica. In some experimental runs, O_2 was provided as the terminal electron acceptor (TEA), whereas in others, O_2 was removed from the systems and Fe(III) in NAu-1 was the only TEA. Experimental solutions were investigated using aqueous chemical techniques and the solid phases were investigated using transmission electron microscopy (TEM). The experimental systems yielded a variety of secondary phases as described elsewhere (O'Reilly et al., 2005). For this report, we focus on the rapid biomineralization of amorphous silica.

2. Experimental procedure

2.1. Starting materials

Nontronite NAu-1 (Clay Minerals Society Source Clays Repository) is a ferruginous ($4.50 \text{ mmol Fe g}^{-1}$) smectite from the Uley Graphite Mine in Australia (Keeling et al., 2000). Tetrahedral layers of NAu-1 contain Si and Al, whereas octahedral layers predominantly contain Fe with some Al and Mg (Gates et al., 2002). Dissolution of smectite in aqueous solutions liberates Si from the clay structure so that it may interact with microorganisms and related biomolecules (O'Reilly et al., 2006). NAu-1 was ground, size-fractionated, and freeze dried prior to use. Only the $<0.2 \mu\text{m}$ fraction was used for the experiments reported here, ensuring 99% purity (Keeling et al., 2000). Prior to each experiment, a required amount of size-fractionated NAu-1 was sterilized by microwave radiation, and sterility was confirmed with the lack of bacterial growth in Luria-Bertani (LB) agar after 24 h.

A minimal culture medium (i.e., M1 medium), adapted from Myers and Nealson (1988), was used in our experiments. This medium has a chemical composition (Appendix A) that is better defined than other culture media commonly used with *S. oneidensis* such as LB medium. It was specifically developed for the cultivation of *S. oneidensis* (Kostka and Nealson, 1998), and has been successfully employed by previous studies of ferruginous clay-*S. oneidensis* incubations (Kostka et al., 1996, 1999a,b; Dong et al., 2003). For experiments reported here, M1 was diluted to 25% in an attempt to minimize the background concentrations of ions such as Fe, Mg, and Ca without compromising the viability of bacteria.

Shewanella oneidensis strain MR-1, a facultative anaerobe capable of dissimilatory iron reduction (Myers and Nealson, 1988), was used for this study as the model dissimilatory iron reducing bacteria. Prior to each experiment, the bacteria, cultured aerobically in LB media, were diluted into fresh LB media and cultured under continuous 200 rpm shaking at room temperature to a concentration of 1.77×10^8 cells mL⁻¹ (measured by optical density at a wavelength of 600 nm). Cultures were then washed twice and resuspended in 25% M1 before the start of each experiment. For experimental runs lacking viable bacteria, the bacterial suspension was heat-killed using microwave radiation prior to the start of the experiment. Sterility was confirmed by lack of growth on LB agar.

2.2. Batch experiments

Forty milligrams of N Au-1 was added to sterile polypropylene centrifuge tubes and microwave sterilized. Forty milliliters of 25% M1 with 5 mM lactate and bacterial suspension was then added. Anaerobic, live culture systems and a series of control systems were prepared that included: (1) anaerobic systems with viable bacteria, (2) anaerobic systems with heat-killed bacteria cells, (3) aerobic systems with viable bacteria, and (4) abiotic systems that contained the same N Au-1 and aqueous media components, but neither viable or killed bacterial cells. All batch experiments were conducted at 23 °C (i.e., ambient room temperature). For each experimental setting, three to four tubes were sacrificed at 4, 24, 48, and 168 h for solid and solution analyses as follows. Each tube was centrifuged at 4500 rpm for 10 min, and 7 mL of the supernatant was removed using a pipette, filtered with 0.2 µm pore size syringe filters, and analyzed for dissolved metal concentrations (e.g., Ca, K, Mg, P, Si, Fe, and Al) using inductively coupled plasma atomic emission spectroscopy (ICP). After pH analysis with a combination electrode calibrated with NBS buffers, the remainder of the sample was saved to determine the extent of Fe reduction using the ferrozine method (Viollier et al., 2000; Washington et al., 2004) as described elsewhere (O'Reilly et al., 2005). Alkalinity was determined spectrophotometrically (Sarazin et al., 1999). Samples for transmission electron microscopy (TEM) analysis were collected and prepared as described in the later section. Bacterial population counts were estimated for the live, anaerobic systems using SYBR Green I fluorescent microscopy (Skeidsvoll and Ueland, 1995); the counts yielded 1.4×10^8 at time zero and 1.2×10^8 , 1.1×10^8 , 8.4×10^8 , and 1.4×10^8 cells mL⁻¹ at 4, 24, 48, and 168 h, respectively.

2.3. Sample preparation for transmission electron microscopy (TEM)

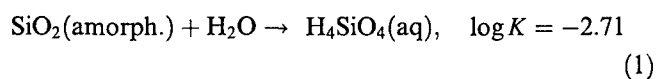
Samples were prepared for TEM analysis as follows using the solid suspensions from batch experiments. After centrifugation, supernatant was removed, and a 5 µl

aliquot of the remaining solid suspension was transferred to a BEEM[®] capsule filled with 50 µl of prepared Nanoplast resin using a pipette. Nanoplast is a hydrophilic melamine resin that has been successfully used to prepare aqueous suspensions of organoclay complexes for TEM ultrathin sectioning (Perret et al., 1991; Wilkinson et al., 1999; Webb et al., 2000; Mondini et al., 2002). It is suited for high-resolution microscopy work in which the structural preservation of bacterial cell surfaces is important. For the preparation of sediments and colloidal suspension in non-marine, low ionic strength aqueous environments, Nanoplast embedding yields high quality ultrathin sections free of extraction artifacts with minimal disturbance to the structural integrity (Perret et al., 1991; Swartz et al., 1997). Nanoplast has also been successfully used for the microstructural preservation of marine organoclay colloids (i.e., marine snow) and microbial communities associated with marine stromatolites without mineral precipitation visible under TEM or confocal microscopy (Heissenberger et al., 1996; Leppard et al., 1996; Decho and Kawaguchi, 1999; Kawaguchi and Decho, 2002). Specifically, Nanoplast has not been found to contribute to undesirable post-sampling deposition or polymerization of silicic acid and other precipitated phases on bacterial cells within marine snow structures rich in diatom fragments (Heissenberger et al., 1996). For our samples, we followed the preparation procedure detailed by Leppard and coworkers for the preparation of marine snow (Leppard et al., 1996): the resin mixture was allowed to slowly replace interstitial water in a 40 °C oven for 2 days, and subsequently cured at 65 °C for 2 days. The use of stain was avoided to ensure that nanometer-scale features composed of light elements (e.g., individual amorphous silica globules) do not become masked by highly electron dense features such as stained organic matter. The Nanoplast-embedded sample was ultrathin-sectioned, and examined with JEOL3010 TEM with Noran energy-dispersive X-ray spectroscopy (EDXS) and selected area electron diffraction (SAED).

3. Results

3.1. Aqueous chemistry

Compositions of the aqueous solutions are shown in Table 1. Temporal evolution of the concentrations of dissolved Si (as determined by ICP) is shown in Fig. 1, together with the solubility of amorphous Si at 25 °C, using the solubility value included in the phreeqc.data database (Parkhurst and Appelo, 1999):



Note that the solubility of SiO₂(amorph.) is effectively independent of pH within the pH range observed for our systems (i.e., 4.19 < pH < 7.55) as the first dissociation constant of H₄SiO₄ (pK₁) is 9.83.

Table 1
Aqueous chemistry of experimental systems

Sample ID	Description	Run (h)	Ca(M)	K(M)	Mg(K)	Si(M)	P(M)	Total Fe (M)	Fe(II) (M)	Fe(III) (M)	Al(M)	pH	Alkalinity (eq)
Initial media													
200	Anoxic live	4	5.90E-04	2.16E-03	2.82E-04	1.62E-05	1.62E-03	2.92E-06			BDL	7.00	6.74E-03
201	Anoxic live	4	6.06E-04	2.18E-03	4.45E-04	4.22E-04	1.66E-03	1.68E-06			BDL	7.44	7.55E-03
202	Anoxic live	4	6.06E-04	2.18E-03	4.51E-04	4.42E-04	1.66E-03	1.45E-06			4.93E-06	7.18	7.87E-03
203	Anoxic live	4	6.02E-04	2.18E-03	4.51E-04	4.09E-04	1.78E-03	1.51E-06			4.66E-06	7.20	7.87E-03
204 ^a	Anoxic live	24	6.21E-04	2.17E-03	4.57E-04	4.53E-04	1.72E-03	1.75E-06	6.00E-07	3.08E-06	3.90E-06	7.20	6.74E-03
205	Anoxic live	24	5.49E-04	1.92E-03	4.08E-04	7.72E-04	1.48E-03	3.68E-06			3.70E-06	7.01	7.07E-03
206	Anoxic live	24	5.78E-04	2.01E-03	4.33E-04	8.09E-04	1.60E-03	8.98E-06			4.54E-06	7.05	6.25E-03
207	Anoxic live	24	5.87E-04	2.14E-03	4.44E-04	8.20E-04	1.61E-03	8.44E-06			3.65E-06	7.31	6.74E-03
208 ^a	Anoxic live	24	6.90E-04	2.74E-03	5.29E-04	9.41E-04	2.00E-03	8.52E-06			6.21E-06	7.55	6.58E-03
209	Anoxic live	48	5.82E-04	1.96E-03	4.40E-04	1.11E-03	1.60E-03	1.62E-05	8.00E-07	1.54E-05	5.99E-06	7.02	7.23E-03
210	Anoxic live	48	5.69E-04	1.97E-03	4.33E-04	1.08E-03	1.65E-03	1.41E-05			4.14E-06	7.02	7.23E-03
211	Anoxic live	48	5.83E-04	1.99E-03	4.41E-04	1.10E-03	1.64E-03	1.36E-05			5.72E-06	7.07	7.39E-03
212 ^a	Anoxic live	48	5.90E-04	2.05E-03	4.49E-04	1.09E-03	1.67E-03	1.37E-05			5.05E-06	7.09	6.74E-03
213	Anoxic live	168	6.37E-04	2.01E-03	4.94E-04	1.69E-03	1.75E-03	1.84E-05	6.00E-07	1.78E-05	3.51E-06	6.81	7.07E-03
214	Anoxic live	168	6.55E-04	1.89E-03	4.93E-04	1.70E-03	1.74E-03	2.27E-05			BDL	6.90	6.74E-03
216	Anoxic live	168	6.14E-04	1.92E-03	4.69E-04	1.66E-03	1.72E-03	2.02E-05			BDL	7.11	6.74E-03
216	Anoxic killed	4	5.73E-04	2.03E-03	4.26E-04	4.19E-04	1.61E-03	7.10E-06			4.58E-06	6.91	6.09E-03
217	Anoxic killed	4	6.21E-04	2.15E-03	4.65E-04	4.55E-04	1.83E-03	1.62E-06			BDL	6.93	9.93E-03
218	Anoxic killed	4	6.12E-04	2.12E-03	4.59E-04	4.60E-04	1.80E-03	1.63E-06			4.04E-06	6.92	6.74E-03
219 ^a	Anoxic killed	24	4.92E-04	1.67E-03	3.60E-04	7.40E-04	1.51E-03	1.48E-06	BDL	1.48E-06	3.48E-06	6.84	6.91E-03
220	Anoxic killed	24	5.81E-04	2.12E-03	4.35E-04	8.40E-04	1.81E-03	1.80E-06			4.10E-06	6.90	6.91E-03
221	Anoxic killed	24	5.85E-04	2.17E-03	4.32E-04	9.06E-04	1.75E-03	1.79E-06			5.13E-06	6.72	6.91E-03
222 ^a	Anoxic killed	48	6.45E-04	2.30E-03	4.54E-04	1.24E-03	1.88E-03	1.42E-06	BDL	1.42E-06	BDL	6.88	6.91E-03
223	Anoxic killed	48	5.87E-04	2.26E-03	4.29E-04	1.10E-03	1.71E-03	2.41E-06			4.18E-06	6.87	6.09E-03
224	Anoxic killed	48	6.00E-04	2.24E-03	4.36E-04	1.17E-03	1.77E-03	2.51E-06			5.87E-06	6.89	6.58E-03
225 ^a	Anoxic killed	168	6.20E-04	2.18E-03	4.43E-04	1.70E-03	1.81E-03	2.01E-05	3.80E-06	1.63E-05	6.63E-06	6.81	8.83E-03
226	Anoxic killed	168	6.06E-04	2.14E-03	4.36E-04	1.58E-03	1.82E-03	1.33E-05			7.90E-06	6.81	5.92E-03
227	Anoxic killed	168	5.94E-04	2.04E-03	4.42E-04	1.62E-03	1.65E-03	8.71E-06			4.58E-06	6.76	6.25E-03
228	Oxic live	4	7.32E-04	2.27E-03	5.23E-04	3.18E-04	1.77E-03	1.89E-05			2.20E-05	4.19	4.59E-03
229	Oxic live	4	6.75E-04	2.46E-03	5.01E-04	2.59E-04	1.77E-03	1.32E-05			2.18E-05	4.20	4.59E-03
230	Oxic live	4	6.99E-04	2.44E-03	5.04E-04	2.81E-04	1.72E-03	1.20E-05			2.18E-05	4.40	4.76E-03
231 ^a	Oxic live	24	7.54E-04	2.39E-03	5.40E-04	6.71E-04	1.72E-03	1.34E-05	1.10E-06	1.23E-05	1.89E-05	4.29	4.93E-03
232 ^a	Oxic live	24	7.44E-04	2.44E-03	5.33E-04	6.60E-04	1.76E-03	1.59E-05	BDL	1.91E-05	1.59E-05	4.30	4.59E-03
233	Oxic live	24	7.63E-04	2.44E-03	5.46E-04	6.95E-04	1.67E-03	1.54E-05			2.36E-05	4.33	5.10E-03
234	Oxic live	48	7.85E-04	2.41E-03	5.64E-04	1.03E-03	1.63E-03	1.56E-05			8.75E-06	4.32	3.75E-03
235 ^a	Oxic live	48	8.19E-04	2.44E-03	5.80E-04	1.01E-03	1.76E-03	1.56E-05	BDL	1.56E-05	2.03E-05	4.24	4.26E-03
236	Oxic live	48	6.27E-04	2.49E-03	4.85E-04	6.88E-04	1.78E-03	1.60E-05			2.06E-05	4.19	4.09E-03
237 ^a	Oxic live	168	7.73E-04	2.47E-03	6.33E-04	1.59E-03	1.83E-03	1.64E-05	7.00E-07	1.57E-05	9.65E-06	5.12	5.10E-03
238	Oxic live	168	8.61E-04	2.54E-03	6.92E-04	1.76E-03	1.82E-03	1.86E-05			8.68E-06	4.77	5.26E-03
239	Oxic live	168	7.99E-04	2.57E-03	6.35E-04	1.64E-03	1.74E-03	1.87E-05			1.39E-05	4.76	5.76E-03
240	Anoxic sterile	4	5.79E-04	2.13E-03	4.58E-04	4.29E-04	1.63E-03	1.91E-05			6.25E-06	7.17	6.58E-03
241	Anoxic sterile	4	6.01E-04	2.18E-03	4.72E-04	4.38E-04	1.67E-03	1.30E-06			7.33E-06	7.19	7.23E-03
242	Anoxic sterile	4	6.40E-04	2.11E-03	4.93E-04	4.74E-04	1.62E-03	1.25E-06			5.89E-06	7.19	6.42E-03
243	Anoxic sterile	24	5.90E-04	2.05E-03	4.66E-04	9.25E-04	1.66E-03	1.51E-06			4.31E-06	7.22	6.74E-03
244	Anoxic sterile	24	5.58E-04	2.11E-03	4.51E-04	8.41E-04	1.71E-03	1.37E-06			5.44E-06	7.27	7.07E-03
245	Anoxic sterile	24	5.34E-04	2.12E-03	4.40E-04	9.66E-04	1.77E-03	1.33E-06			6.27E-06	7.22	5.76E-03
246	Anoxic sterile	48	5.62E-04	2.00E-03	4.49E-04	1.26E-03	1.76E-03	1.35E-06			7.56E-06	7.17	5.92E-03
247	Anoxic sterile	48	5.52E-04	2.07E-03	4.47E-04	1.21E-03	1.72E-03	1.48E-06			4.95E-06	7.23	6.58E-03
248	Anoxic sterile	48	5.58E-04	2.08E-03	4.50E-04	1.27E-03	1.70E-03	1.46E-06			4.67E-06	7.20	6.42E-03
249	Anoxic sterile	168	4.70E-04	1.67E-03	3.62E-04	1.37E-03	1.38E-03	1.51E-06			6.52E-06	7.18	5.92E-03
250	Anoxic sterile	168	4.91E-04	2.12E-03	4.19E-04	1.50E-03	1.77E-03	2.38E-06			6.38E-06	7.23	6.25E-03
251	Anoxic sterile	168	5.32E-04	2.00E-03	4.26E-04	1.69E-03	1.68E-03	4.03E-06			8.09E-06	7.19	5.92E-03

All reported values are from ICP analysis except for some Fe. BDL for Al, below detection limit (i.e., $<3.07 \times 10^{-6}$ M). BDL for Fe(II), below detection limit (i.e., $<4.0 \times 10^{-7}$ M).

^a In selected samples, Fe(II) and total Fe (Fe(II) + Fe(III)) were determined using Ferrozine method, and Fe(III) was derived by difference.

Temporal evolution of the bulk saturation indices (SI) for amorphous silica, non-crystalline ferric oxyhydroxide (represented as Fe(OH)₃(am)), and NAu-1 with Ca end-member is shown in Table 2. The SI values for bulk

aqueous phases were determined using the PHREEQC code and phreeqc.data database (Parkhurst and Appelo, 1999). In addition to the thermodynamic constants provided in the database phreeqc.data, stability constants of

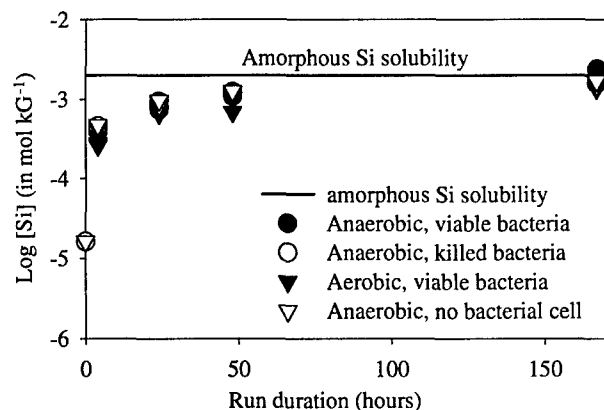


Fig. 1. Evolution of the dissolved Si concentration in our experimental systems. The equilibrium concentration for amorphous silica, calculated by assuming that aqueous Si concentration is fully attributed to monomeric silica (i.e., $\text{H}_4\text{SiO}_4(\text{aq})$, H_3SiO_4^- , etc.), is shown for comparison. All systems were apparently undersaturated with respect to amorphous silica at least for the first 48 h. They became very close to saturation after 7 days.

relevant metal- and proton-EDTA complexes and metal- and proton-lactate complexes (Table 3) were used in the calculations. Lactate and EDTA concentrations were taken from the 25% dilution of M1 medium (Appendix A). Note that phreeqc.data database assumes all dissolved silica to be in the monomeric form (i.e., $\text{H}_4\text{SiO}_4(\text{aq})$, H_3SiO_4^- , etc.). Metal-amino acid complexes were not considered because: (i) systematic stability constants are not available for key metal species in our systems; and (ii) preliminary PHREEQC calculations using available stability constants (e.g., Al(III) and Fe(III)-serine complexes (Djurdjevic and Jelic, 1997; Dayde et al., 2002)) indicated that the concentrations of metal-amino acid complexes would be several orders of magnitudes less than the metal-EDTA complexes in the pH range relevant to this study. Gibbs free energy of formation for NAu-1 was estimated using the method recently detailed by (Vicillard, 2000). Its dissolution constant was subsequently calculated using the estimated ΔG_f^0 value (Table 3). Solution concentrations tabulated in Table 1 were used as input. For major species not listed in Table 1 (e.g., Na, SO_4^{2-}), concentration values were estimated to be consistent with the initial 25% media composition (i.e., 25% of the values listed in Appendix A). Determination of dissolved Fe(II)-Fe(III) ratio was conducted on selected samples only (Table 1). Consequently, the ratio determined for the selected sample was assumed to prevail for other samples with the same experimental conditions (i.e., oxygen availability, bacteria viability, and run duration). For example, Fe(II)-Fe(III) ratio found in Run ID#204 (i.e., 0.16-0.84) was assumed to be also valid for Run ID#205, 206, and 207 (see Table 1). None of the 4 h runs nor initial media were analyzed for Fe(II)-Fe(III) ratio. Consequently, we assumed that all dissolved Fe in the aqueous phase of 4 h runs and initial media was in the form of Fe(III), regardless of the oxygen content or bacteria viability. The Fe(III)-(Fe(II) + Fe(III)) ratio in

our experiments are consistent with a recent finding that Fe(III) reduction by *S. oneidensis* is very slow when Fe(III) is chelated by strong chelators such as EDTA (Haas and DiChristina, 2002).

3.2. TEM observations of amorphous Si

Amorphous silica precipitates were detected in all of the experimental systems with run durations of 24 h to 7 days that contained *S. oneidensis*, including the systems in which bacteria had been heat-killed prior to $t = 0$. In most observed instances, amorphous silica was present as clusters of small (i.e., <50 nm) globules (Figs. 2-4). In many cases, the clusters exhibited intimate spatial associations with bacterial cells or EPS, whereas in other cases the clusters were discrete. These features were confirmed to be Si-rich with EDXS, whereas their amorphous nature was verified by SAED (not shown). EDXS spectra also show that they were very low in other cations including trivalent cations (i.e., Al and Fe) that were found in previous studies to act as bridging cations between bacterial cell surfaces and monosilicic acid (Fein et al., 2002). Amorphous silica was not detected in the sterile experimental systems free of bacterial cells and associated biomolecules.

4. Discussion

Rapid (i.e., within 24 h) precipitation of amorphous silica globules occurred in aqueous solutions that appeared to be slightly undersaturated with respect to amorphous silica at the expense of dissolving NAu-1. The apparent undersaturation was determined by assuming all dissolved silica was in the monomeric form (Fig. 1). However, if the metastable equilibrium between amorphous silica and polysilicic acids, rather than monomeric silica, is considered, our experimental systems can be regarded as supersaturated with respect to amorphous silica. A significant portion of the aqueous silica measured in our systems may have been in the form of polysilicic acids because aqueous silica was exclusively supplied through the concurrent dissolution of NAu-1. TEM analysis of solid samples revealed abundant amorphous silica globules that were often found in the immediate vicinity of bacterial cells or EPS. Amorphous silica was the predominant solid phase immediately associated with the bacterial cells and EPS, although other phases were also detected under TEM (O'Reilly et al., 2005).

4.1. Source of silica

Concentration of dissolved Si increased with time in our experimental systems (Fig. 1). This is due to the dissolution of NAu-1. The initial media used in all experiments was undersaturated with respect to NAu-1 (i.e., $\text{SI} < -2.5$, see Table 3) thus NAu-1 dissolution was thermodynamically expected. However, after 4 h, all bulk aqueous phases became apparently supersaturated with respect to NAu-1, except for the aerobic systems with viable bacteria (i.e., Run

Table 2
Saturation indices (SI)

Sample ID	Description	Run (h)	Amorphous Si	Fe(OH) ₃ (am)	Ca-NAu-1
Initial media		0	-2.08	-2.99	Less than -2.5
200	Anoxic live	4	-0.66	-1.32	Less than 5.8
201	Anoxic live	4	-0.64	-2.15	4.47
202	Anoxic live	4	-0.67	-2.08	4.47
203	Anoxic live	4	-0.63	-1.99	4.74
204	Anoxic live	24	-0.40	-2.28	4.97
205	Anoxic live	24	-0.38	-1.52	6.53
206	Anoxic live	24	-0.37	-0.81	7.78
207	Anoxic live	24	-0.31	-0.04	9.56
208	Anoxic live	48	-0.24	-0.10	9.72
209	Anoxic live	48	-0.25	-0.84	8.19
210	Anoxic live	48	-0.24	-0.79	8.40
211	Anoxic live	48	-0.25	-0.71	8.51
212	Anoxic live	168	-0.06	1.39	12.95
213	Anoxic live	168	-0.06	2.06	Less than 14.2
214	Anoxic live	168	-0.07	1.93	Less than 13.9
216	Anoxic killed	4	-0.66	-2.04	4.55
217	Anoxic killed	4	-0.63	-2.82	Less than 3.1
218	Anoxic killed	4	-0.62	-2.84	3.17
219	Anoxic killed	24	-0.42	-3.20	3.10
220	Anoxic killed	24	-0.36	-2.87	4.02
221	Anoxic killed	24	-0.33	-3.34	3.20
222	Anoxic killed	48	-0.19	-3.00	Less than 4.3
223	Anoxic killed	48	-0.24	-2.80	4.56
224	Anoxic killed	48	-0.22	-2.70	4.93
225	Anoxic killed	168	-0.06	0.53	11.54
226	Anoxic killed	168	-0.09	-1.60	7.55
227	Anoxic killed	168	-0.08	-2.33	6.01
228	Oxic live	4	-0.77	-4.02	-3.11
229	Oxic live	4	-0.86	-5.95	-7.02
230	Oxic live	4	-0.83	-5.56	-5.71
231	Oxic live	24	-0.45	-5.91	-5.33
232	Oxic live	24	-0.46	-5.00	-3.60
233	Oxic live	24	-0.44	-5.20	-3.76
234	Oxic live	48	-0.27	-5.39	-3.84
235	Oxic live	48	-0.27	-5.28	-3.58
236	Oxic live	48	-0.44	-5.25	-4.26
237	Oxic live	168	-0.08	-3.03	3.08
238	Oxic live	168	-0.04	-2.59	3.25
239	Oxic live	168	-0.07	-2.58	3.27
240	Anoxic sterile	4	-0.65	1.88	11.91
241	Anoxic sterile	4	-0.64	-2.17	4.53
242	Anoxic sterile	4	-0.61	-2.16	4.62
243	Anoxic sterile	24	-0.32	-2.02	5.79
244	Anoxic sterile	24	-0.36	-1.95	5.83
245	Anoxic sterile	24	-0.30	-2.13	5.75
246	Anoxic sterile	48	-0.19	-2.24	6.00
247	Anoxic sterile	48	-0.20	-2.03	6.20
248	Anoxic sterile	48	-0.18	-2.12	6.10
249	Anoxic sterile	168	-0.15	-2.23	6.09
250	Anoxic sterile	168	-0.11	-1.85	6.92
251	Anoxic sterile	168	-0.06	-1.64	7.56

[Al(III)] was below detection limit in some systems. Upper limit values for SI for NAu-1 in those systems were estimated by assuming [Al(III)] = 3.07 μM which was the detection limit.

#228–236). Despite the apparent supersaturation, Si continued to partition into aqueous phases. Clearly, the description of aqueous phase chemistry that was used in conjunction with PHREEQC does not accurately represent the environment that surrounded NAu-1 in our experiments.

It has been reported that dissolution of aluminosilicates at ambient temperature first yields polysilicic acids rather than thermodynamically stable monosilicic $\text{H}_4\text{SiO}_4(\text{aq})$ (Dietzel, 2000). The sole source of silica in our experimental systems was NAu-1, an aluminosilicate mineral. Thus, a portion of the total dissolved silica in each of our systems

Table 3
Thermodynamic constants used in conjunction with PHREEQC calculations

Reaction	Log <i>K</i>	Reference
$H^+ + EDTA^{4-} = HEDTA^{3-}$	10.21	a
$H^+ + HEDTA^{3-} = H_2EDTA^{2-}$	6.18	a
$H^+ + H_2EDTA^{2-} = H_3EDTA^-$	2.78	a
$H^+ + H_3EDTA^- = H_4EDTA(aq)$	2.1	a
$Fe^{3+} + H_2EDTA^{2-} = FeEDTA^- + 2H^+$	8.6	a
$Al^{3+} + H_2EDTA^{2-} = AlEDTA^- + 2H^+$	0.1	a
$Ca^{2+} + H_2EDTA^{2-} = CaEDTA^{2-} + 2H^+$	-5.87	a
$Mg^{2+} + H_2EDTA^{2-} = MgEDTA^{2-} + 2H^+$	-7.56	a
$Mn^{2+} + H_2EDTA^{2-} = MnEDTA^{2-} + 2H^+$	-2.58	a
$Zn^{2+} + H_2EDTA^{2-} = ZnEDTA^{2-} + 2H^+$	0.05	a
$H^+ + Lact^- = HLact(aq)$	3.86	b
$Fe^{3+} + Lact^- = FeLact^{2+}$	6.4	b
$Al^{3+} + Lact^- = AlLact^{2+}$	2.48	b
$Ca^{2+} + Lact^- = CaLact^+$	1.23	b
$Mg^{2+} + Lact^- = MgLact^+$	0.93	b
$Mn^{2+} + Lact^- = MnLact^+$	1.19	b
$Zn^{2+} + Lact^- = ZnLact^+$	1.86	b
$Ca_{0.26}Mg_{0.02}Si_3.4925Al_{0.65}Fe_{1.84}O_{10}(OH)_2 + 8.03H^+ + 1.97H_2O = 0.26Ca^{2+} + 0.02Mg^{2+} + 3.4925H_4SiO_4 + 0.65Al^{3+} + 1.84Fe^{3+}$	-1.57	Calculated using ΔG_f^0 below
NAu-1 (Ca end-member) Formula: $Ca_{0.26}Mg_{0.02}Si_3.4925Al_{0.65}Fe_{1.84}O_{10}(OH)_2$ $\Delta G_f^0: -4640 \text{ kJ mol}^{-1}$		c d

Lact⁻ denotes lactate ion, CH₃CH(OH)COO⁻.

^a Hovey and Tremaine (1985).

^b Portanova et al. (2003).

^c Keeling et al. (2000).

^d Vieillard (2000).

may have been maintained as polysilicic acids due to the balance between continuous polysilicic acid production (due to ongoing NAu-1 dissolution) and thermodynamically favored depolymerization. In typical circumneutral natural waters, depolymerization occurs within a few hours to a day (Dietzel, 2000). However, it has been reported that subsequent depolymerization of polysilicic acid to H₄SiO₄(aq) is substantially slowed down when a small amount of phosphate is present in the aqueous solutions (e.g., 35% decrease in the depolymerization rate with 50 μmol L⁻¹ HPO₄²⁻ concentration) (Dietzel and Usdowski, 1995), even though the mechanisms for polysilicic acid stabilization are not yet understood. The half life of polysilicic acid has been empirically expressed as a function of phosphate concentration as follows:

$$t_{1/2} = \frac{1}{[p - Si]_i k_D'} \quad (2)$$

where: $k_D' = \alpha \cdot k_D$ (unit: (mol/L)⁻¹s⁻¹), $k_D = \text{pH}^{11.61} \cdot 5.614 \times 10_{-10}$,

$\alpha = \exp(A \cdot (\exp([HPO_3^{2-}] \cdot B) - \exp([HPO_3^{2-}] \cdot C)))$

$A = 0.2567$, $B = -0.00004$, $C = 11000$

$[p - Si]_i$, portion of initial Si concentration attributed to polysilicic acid (Dietzel and Usdowski, 1995; Dietzel, 2000). Using these empirical relationships together with the measured pH and $\Sigma[PO_3]$, and the PHREEQC-derived $\Sigma[PO_3]$ speciation, we obtain the k_D' value for

each experimental condition as shown in Table 4. These k_D' values lead to the half life of polysilicic acid being virtually infinite regardless of $[p - Si]$ values except for the oxic live systems. Note that the empirical relationship above was derived for the $[HPO_3^{2-}]$ concentrations below 0.1 mM, whereas $[HPO_3^{2-}]$ concentration values in our systems are approximately one order of magnitude greater. Consequently, the half lives estimated here contain very large uncertainty. However, it is still likely, for all of our experimental systems except for the aerobic systems with viable bacteria, that: (i) polysilicic acid depolymerization was extremely slow; and (ii) virtually all dissolved Si remained as polysilicic acid during the duration of the experimentals. In addition to the effect of phosphate, polysilicic acid depolymerization is expected to be further hindered by the presence of biomolecules associated with bacterial metabolism (see Section 4.2 below). Dissolved phosphate concentrations of ~50 μM or greater have been documented from a range of environments including marine and freshwater sediments and soils; the phosphate is generated from organic matter degradation or weathering of phosphorus-rich rocks (Goldhaber et al., 1977; Jahnke et al., 1983; Sundby et al., 1992; Moore and Reddy, 1994; Follmi, 1996; Taunton et al., 2000). Consequently, it is likely that conditions favorable for the stabilization of polysilicic acids could be found in many modern and ancient environments.

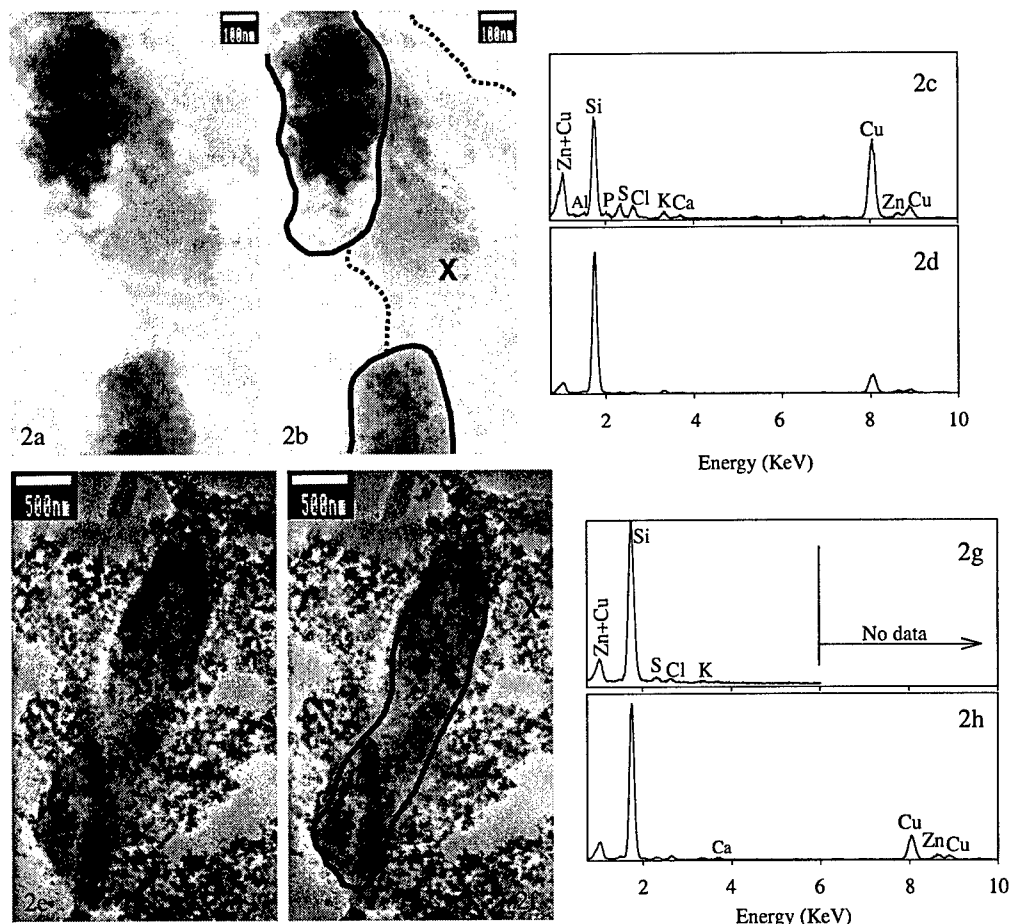


Fig. 2. Clusters of amorphous Si globules were observed in the immediate vicinity of EPS and bacterial cells in samples sacrificed after 24 h of anaerobic incubation with viable cells. The globules are typically less than 50 nm in diameter. Their amorphous nature was confirmed by SAED (not shown). The globules are virtually free of other ions, indicated by EDXS spectra. Zinc and copper signals in EDXS are from the sample holder material. (a) A TEM bright field image showing two ~250 nm clusters of small amorphous silica globules and EPS in between. Each globule is approximately 30–40 nm in diameter. (b) An identical field of image to (a), while illustrating the approximate outline of the clusters (solid lines) and EPS (broken lines), and approximate beam locations for the EDXS analysis. (c) An EDXS spectrum taken from EPS that is closely associated with amorphous silica globules. The approximate beam location is indicated by "X" in (b). Strong Si signals were obtained together with signals from elements typically found in bacterial cells and associated biomolecules, such as P, S, K, and Ca (Norland et al., 1995; Heldal et al., 2003). Zinc and Cu signals are from the sample mounting material. (d) An EDXS spectrum taken from a silica cluster. The approximate location is indicated by "Y" in (b). Signals from biomolecule-related elements are much weaker than those seen in (c). (e) A TEM bright field image showing a massive cluster of small (~30–50 nm) amorphous silica globules assembled around what appears to be a rod-shaped bacterial cell (approximately 3 μm long and 0.7 μm wide). (f) An identical field of image to (e) illustrating the approximate outline of the bacterial cell and beam locations for the EDXS analysis. (g) An EDXS spectrum taken from the cluster of amorphous silica globules. The approximate beam location is indicated by "X" in (f). It is dominated by Si, while small amounts of elements associated with bacterial cells and EPS (i.e., S and K) are also present. (h) An EDXS spectrum taken from the silica-encrusted cell. The approximate beam location is indicated by "Y" in (f). The spectrum is dominated by Si, while small amounts of elements associated with bacterial cells and EPS (i.e., S and Ca) are also present. Virtually no trivalent cations such as Al or Fe were detected.

NAu-1 dissolution continued in our systems even after apparent supersaturation was reached in the bulk solutions, yielding polymerized aqueous Si. Dissolution of NAu-1 despite the apparent supersaturation may be explained by the possible inability of polysilicic acids to directly participate in the NAu-1 precipitation (i.e., reverse) reaction at a rate that is comparable to that of dissolution (i.e., forward) reaction. High levels of supersaturation with respect to smectite have been reported previously in natural aluminosilicate systems with a high degree of biological activities (Kawano and Tomita, 2001, 2002).

4.2. Rapid formation and stabilization of <50 nm amorphous Si globules

Recent extensive investigations of diatom-mediated silica precipitation mechanisms have found that biomolecules produced by diatoms, especially polyamines and peptides with polyamine side chains, induce initial polymerization of H_4SiO_4 monomers (Kroger et al., 1999, 2000; Bauerlein, 2003; Poulsen et al., 2003; Knecht and Wright, 2004). Silica globules with diameters between 40 and 60 nm, much like those observed in our systems in terms of morphology, were found to form *in vitro* in the presence of polyamines

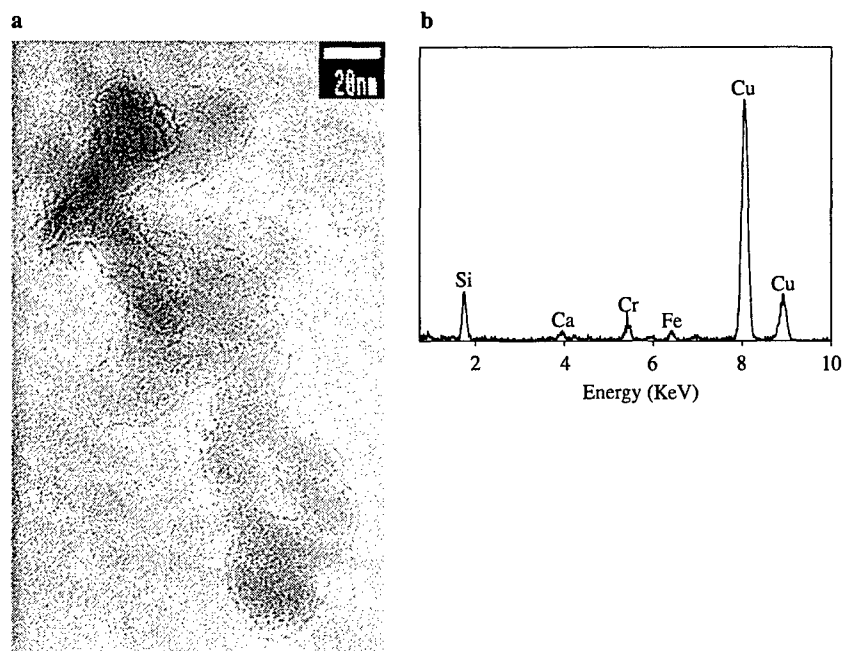


Fig. 3. (a) Cluster of amorphous Si globules were observed in samples sacrificed after 7 days of aerobic incubation with viable cells. Each globule is ~ 20 nm in diameter. Clusters are often associated with bacterial cells but some times found discretely as shown here. (b) EDXS spectrum confirms that the cluster was primarily composed of Si. Chromium signals in the EDXS spectrum are from the TEM sample stage.

(Sumper, 2004; Sumper and Brunner, 2006). When Si-supersaturated solution was mixed with poly(allylamine), which is a polyamine found in certain diatom species, globules of Si (40–60 nm in diameter, depending on pH) appeared within minutes, and remained stable at least for a few days without further Ostwald ripening (Sumper, 2004; Sumper and Brunner, 2006). Electrostatic interactions between negatively charged polysilicic acid and positively charged amino groups that are organized along the polyamine chains have been suggested as a required step for further Si polymerization and subsequent amorphous silica precipitation (Mizutani et al., 1998; Coradin et al., 2002).

Existing *in vitro* investigations of polyamine–Si interaction have focused primarily on long-chain polyamines. However, simpler polyamines, such as putrescine, possess amino groups along the chains and thus can also catalyze Si precipitation from $\text{H}_4\text{SiO}_4(\text{aq})$ solution (Belton et al., 2005). Polyamines are polycationic molecules ubiquitous in all biological materials. In microorganisms, they are produced through decarboxylation of either ornithine, arginine, or lysine (Tabor and Tabor, 1985). Our culture medium (Appendix A) contained 5 mg L^{-1} of arginine, which is one of the three possible precursors for the bacterial polyamines.

Meanwhile, *S. oneidensis* MR-1 as well as *Shewanella putrefaciens*, which is closely related to *S. oneidensis* MR-1 (Venkateswaran et al., 1999), have been recognized to metabolically produce abundant putrescine and other simple polyamines (Lopez-Caballero et al., 2001; Benner et al., 2004; Ghosal et al., 2005). A recent study documented

activities of the gene that encodes arginine decarboxylase in *S. oneidensis* MR-1 using an aqueous culture medium similar to ours, i.e., 100% M1 plus 50 mg L^{-1} tryptone and 25 mg L^{-1} yeast extract (Leaphart et al., 2006). Thus, it is possible that putrescine or another biomolecule with simple polyamine chains produced by *S. oneidensis* MR-1 was present in our experimental systems as well and was essential in the formation as well as the stabilization of <50 nm silica globules.

In most of the bio-inspired, *in vitro* amorphous silica precipitation studies, the Si source was explicitly monomeric H_4SiO_4 which went through the polymerization process from scratch. However, our systems likely supplied Si as polysilicic acid in the first place because Si was supplied by the concurrent dissolution of aluminosilicate. It is possible that amorphous silica precipitation in our systems was very rapid due to the already polymerized Si supply.

4.3. Sorption of Si globules onto *Shewanella oneidensis* cells

In circumneutral pH, aqueous silica is either neutrally charged monosilicic acid (i.e., $\text{H}_4\text{SiO}_4(\text{aq})$), or aqueous polymer or colloidal sol which carries a negative charge in the form of Si-O^- (Coradin and Lopez, 2003). The negative charge remains when further polymerization occurs. Thus, in order for the amorphous silica globules to electrostatically form clusters and chains or to attach to negatively charged surfaces of bacterial cells, the charge must be neutralized or reversed. Previous studies reported that the surface of nanometer-sized silica globules formed and stabilized *in vitro* under the presence of polyamines is

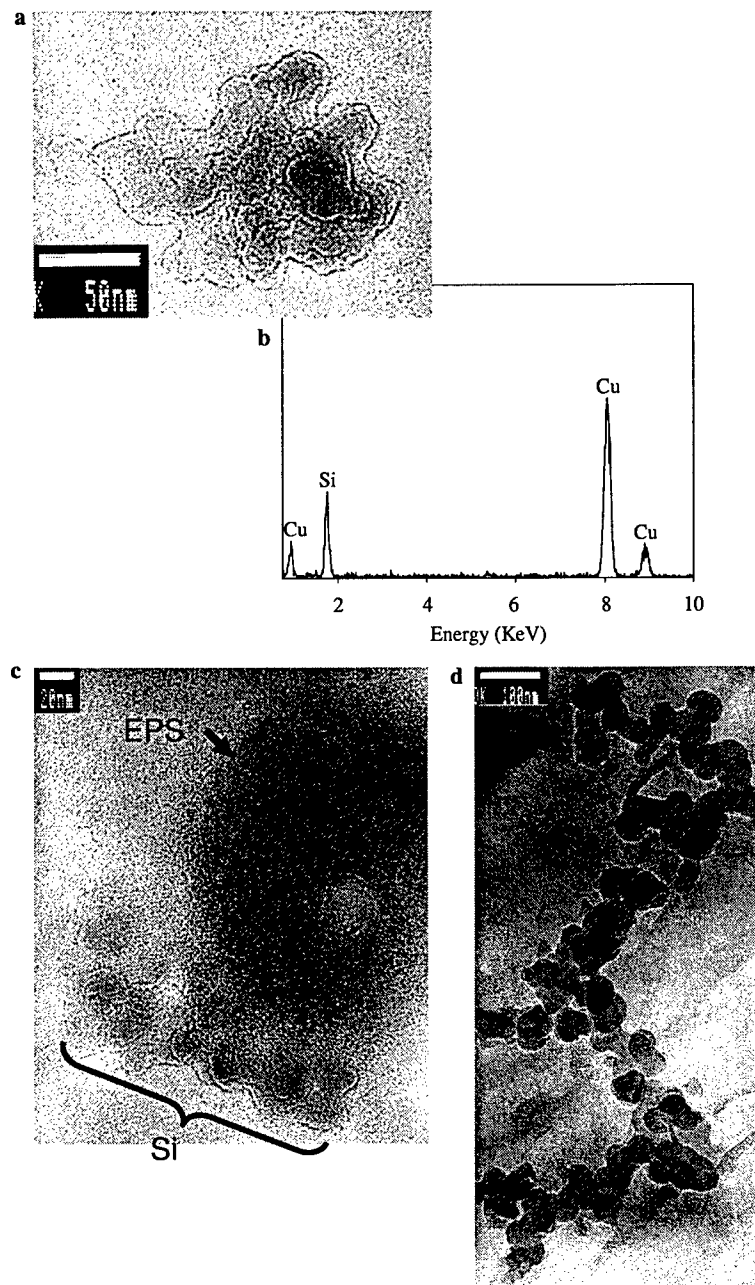


Fig. 4. Clusters of amorphous silica globules were observed in samples sacrificed after 7 days of anaerobic batch incubation with heat-killed cells. (a) A small cluster of amorphous silica globules. (b) The EDXS spectrum taken from the amorphous silica cluster shown in (a). It is dominated by Si signals. (c) Some amorphous silica globules (Si) were in the immediate vicinity of EPS. (d) Some amorphous silica globules were organized into a chain structure.

Table 4
Coefficient for polysilicic acid half life, k'_D

	Measured pH	PHREEQC-derived [HPO ₃ ²⁻] (M)	k'_D
Initial media	7.00	6.21E-4	≈0
Anaerobic live	7.13 ± 0.19	7.65E-4 ± 2.17E-4	≈0
Anaerobic killed	6.85 ± 0.07	5.28E-4 ± 0.70E-4	<10 ⁻³⁶
Oxic live	4.43 ± 0.30	3.83E-6 ± 3.86E-6	1.5 × 10 ⁻²
Anaerobic sterile	7.21 ± 0.03	8.34E-4 ± 0.68E-4	≈0

positively charged; this may be due to strong adsorption (i.e., chemisorption) of organic polycations (such as polyamines) resulting in charge reversal (Iler, 1979; Sumper, 2004; Sumper and Brunner, 2006). Neutrally or negatively charged aqueous/colloidal species do not have affinity to net negatively charged *S. oneidensis* cell surfaces, whereas silica globules that are positively charged due to charge reversal which resulted from chemisorption would be electrostatically attracted to the negatively charged cell surfaces.

In previous studies, experimental silica sorption on bacterial cells in amorphous silica-undersaturated systems was accomplished when the aqueous concentration of Fe(III) exceeded the saturation value of ferric oxyhydroxides (approximately >0.02 mM Fe(III)), or when bacteria cells were deliberately modified with ferric oxyhydroxide precipitates or sorbed cations (Urrutia and Beveridge, 1994; Fein et al., 2002; Phoenix et al., 2003). In our experiments, amorphous silica globules in association with cells and EPS were found in systems with low aqueous Fe(III) that are undersaturated with respect to ferric oxyhydroxides (e.g., the products seen in Fig. 2 were found in live anoxic systems after 24 h of incubation). Electron micrographs of the cation-bridged Si precipitates on *B. subtilis* do not exhibit globule morphology (Mera and Beveridge, 1993). Charge characteristics of gram positive bacteria (such as *B. subtilis*) and gram negative bacteria (such as *S. putrefaciens*) have been found to be qualitatively similar (Jiang et al., 2004; Claessens et al., 2006) thus silica globules that are positively charged due to chemisorption would be attracted equally well to the *B. subtilis* cell surfaces if present. Clearly, in these previously studied systems, silica did not become polyamine-stabilized globules that are positively charged due to chemisorption.

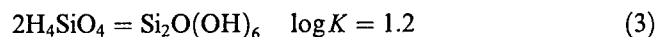
Lack of silica globules in the previous studies may be explained by lower concentrations of polyamines and phosphate in those systems compared to our systems. Additionally, in the previous studies, Si was supplied as dissolved monomeric H_4SiO_4 rather than as polysilicic acids. Our aqueous solutions, based on M1 media (diluted to 25%, Appendix A), contained arginine that is essential for the bacterial production of polyamines through arginine decarboxylation (Tabor and Tabor, 1985; Lu, 2006). Even in our heat-killed systems, polyamines were likely to be present because no washing was conducted after the heat treatment. On the other hand, previous studies were conducted with *B. subtilis* cells that were washed twice and suspended in distilled and deionized water (Mera and Beveridge, 1993; Fortin and Ferris, 1998; Fein et al., 2002) that likely contained little arginine or with cyanobacteria suspended in dilute BG11 media which does not contain any amino acids (Yee et al., 2003). Even though microorganisms were viable in the previous experiments, they may have not been producing polyamines due to lack of arginine as the precursor.

4.4. Amorphous silica saturation state

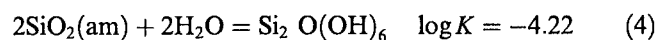
Calculations using phreeqc.data suggest that amorphous silica precipitation occurred in aqueous solutions that were apparently undersaturated with respect to the equilibrium between amorphous silica and monosilicic acid (Table 2). However, these calculations were carried out under the database's built-in assumption that all Si detected in aqueous solutions was monomeric. This assumption does not

accurately depict our systems because our systems likely contained highly polymerized polysilicic acids as the primary aqueous Si species because Si in our systems was supplied by the concurrent dissolution of aluminosilicate clays and because of the presence of phosphate in the systems.

Thermodynamic properties of highly polymerized polysilicic acids are largely unknown. However, the formation constant of disilicic acid has been previously estimated as follows:



(Sjoberg, 1996). Note that $Si_2O(OH)_6$, rather than deprotonated $Si_2O_2(OH)_5^{5-}$, is the predominant dimeric aqueous silica species in our experimental systems as the first dissociation constant of disilicic acid is $10^{8.95}$ (Sjoberg, 1996). By combining Eq. (3) with the solubility of amorphous silica (i.e., Eq. 1), we obtain the solubility of amorphous silica in an environment where disilicic acid is the predominant aqueous Si species:



A stability diagram (Fig. 5) can be derived from this relationship. Concentrations of aqueous Si in all of our experimental products are positioned above the line indicating the metastable equilibrium between amorphous silica and disilicic acid, even though they are below the stability line between amorphous silica and monosilicic acid. Note that the actual experimental systems likely contained a range of aqueous silica species including polysilicic acids, disilicic acid, and monosilicic acid, rather than disilicic acid alone. However, the stability lines for the metastable equilibria between amorphous silica

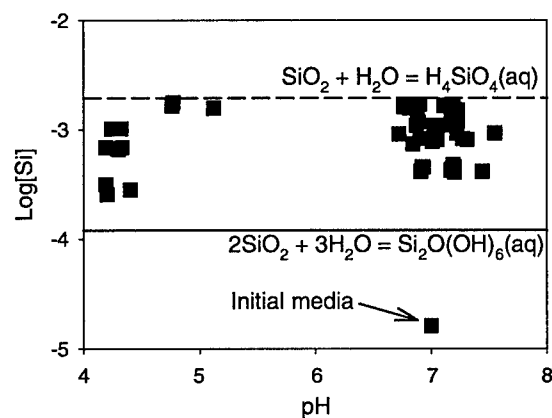


Fig. 5. Stability of amorphous Si is represented as a function of pH and concentration of aqueous Si (mol Si L^{-1}) for two different hypothetical systems: (i) systems in which disilicic acid is the predominant aqueous Si species (solid line); and (ii) systems in which monosilicic acid is the predominant aqueous Si species (broken line). Aqueous Si concentrations measured for our experimental systems (filled squares) are all positioned above the stability field boundary for disilicic acid equilibrium, indicating that the systems were supersaturated with respect to amorphous Si if disilicic acid was the predominant aqueous Si species.

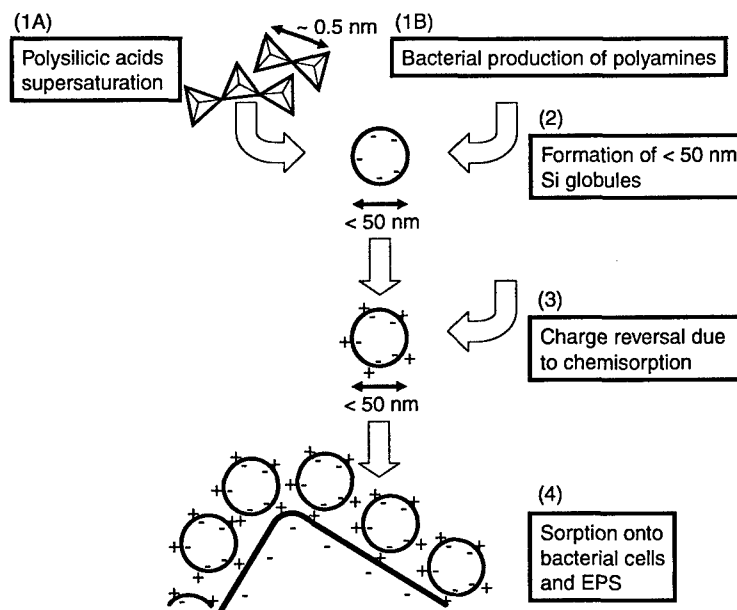


Fig. 6. Proposed mechanism for the formation of observed amorphous silica globules and their association with bacteria and EPS in our experimental systems. (Step 1A) Dissolution of NAu-1 yields supersaturation of aqueous polysilicic acids with respect to amorphous silica; (Step 1B) *Shewanella oneidensis* MR-1 produces polyamines; (Step 2) Polysilicic acids are further polymerized to form <50 nm amorphous silica globules with the help of polyamines; (Step 3) Negatively charged surface of amorphous silica globules become positively charged due to chemisorption; (Step 4) Positively charged amorphous silica globules are sorbed onto net negatively charged surfaces of bacteria and EPS.

and higher order polysilicic acids would be located below those for monosilicic and disilicic acids. Consequently, our experimental systems were most likely supersaturated with respect to amorphous silica as they contained aqueous silica species with a range of polymerization. Thus, silica precipitation occurred, despite the apparent undersaturation derived from the assumption of monosilicic acid predominance.

4.5. Summary of *Shewanella oneidensis*-mediated precipitation of amorphous silica

Proposed mechanism for the *S. oneidensis*-mediated precipitation of amorphous silica is summarized in Fig. 6. Aqueous solutions became supersaturated with respect to the equilibrium between polysilicic acids and amorphous Si (i.e., Step 1A), as aqueous Si in our systems were predominantly polysilicic acids that were produced by dissolving aluminosilicate clays and subsequently stabilized by phosphate (Dietzel, 2000). Production of polyamines (i.e., Step 1B) has been reported for *S. putrefaciens* in the presence of amino acids (Benner et al., 2004). Polyamine-assisted formation and stabilization of <50 nm amorphous silica globules (i.e., Step 2) has been reported to occur in *in vitro* experiments (Sumper, 2004; Sumper and Brunner, 2006). The globules that became positively charged due to chemisorption (i.e., Step 3) (Iler, 1979; Sumper, 2004; Sumper and Brunner, 2006) would then be electrostatically attracted to net negatively charged bacterial cell surfaces and EPS (i.e., Step 4).

In this study, the close spatial association between bacterial cell or EPS and amorphous silica was attained in low Fe(III) solutions in apparently silica-undersaturated systems. Previously, amorphous silica precipitation from aqueous solutions with low dissolved silica concentration was primarily observed when at least ~0.2 mM or more Fe(III) was also present in the system to function as a bridging cation, or when the bacterial surface was deliberately coated with ferrihydrite (Kawano and Tomita, 2001; Fein et al., 2002; Phoenix et al., 2003; Yee et al., 2003). In this study, amorphous silica globules were precipitated in association with bacteria and EPS in apparently undersaturated, low Fe(III) (i.e., <~0.02 mM) solution. This is probably because (i) the aqueous silica supply was already polymerized; and (ii) charge reversal occurred due to chemisorption.

Acknowledgments

This study was funded by ONR/NRL Core 6.1 funding (PE#0601153N). A part of this work was performed while S.E. O'Reilly held a National Research Council Research Associateship award at NRL. S. Newell assisted bacterial cell count. TEM analyses were conducted at NRL Center for Electron Microscopy. ICP analysis was conducted by J. Delcambre at APG Environmental (Stennis Space Center, Mississippi). We thank three anonymous reviewers and Associate Editor Dr. Fein for constructive reviews that helped us substantially improve the manuscript. NRL Contribution JA/7430-04-13.

Associate editor: Jeremy B. Fein

Appendix A

Component	Concentration
Lactate	20 mM
(NH ₄) ₂ SO ₄	9.0 mM
K ₂ HPO ₄	3.3 mM
KH ₂ PO ₄	3.3 mM
NaHCO ₃	2.0 mM
MgSO ₄	1.01 mM
CaCl ₂	0.485 mM
Na ₂ EDTA	67.2 μM
H ₃ BO ₃	56.6 μM
NaCl	10.0 μM
FeSO ₄	5.4 μM
CoSO ₄	5.0 μM
Ni(NH ₄) ₂ (SO ₄) ₂	5.0 μM
Na ₂ MoO ₄	3.87 μM
Na ₂ SeO ₄	1.5 μM
MnSO ₄	1.26 μM
ZnSO ₄	1.04 μM
CuSO ₄	0.2 μM
Arginine	20 mg L ⁻¹
Glutamate	20 mg L ⁻¹
Serine	20 mg L ⁻¹

References

- Asada, R., Tazaki, K., 2001. Silica biomineralization of unicellular microbes under strongly acidic conditions. *Can. Mineralogist* **39**, 1–16.
- Bauerlein, E., 2003. Biomineralization of unicellular organisms: an unusual membrane biochemistry for the production of inorganic nano- and microstructures. *Angew. Chem. Int. Ed.* **42** (6), 614–641.
- Belton, D., Patwardhan, S.V., Perry, C.C., 2005. Putrescine homologues control silica morphogenesis by electrostatic interactions and the hydrophobic effect. *Chem. Commun.* (27), 3475–3477.
- Benner, R.A., Staruszkiewicz, W.F., Otwell, W.S., 2004. Putrescine, cadaverine, and indole production by bacteria isolated from wild and aquacultured penaeid shrimp stored at 0, 12, 24, and 36 degrees C. *J. Food Prot.* **67** (1), 124–133.
- Benning, L.G., Phoenix, V.R., Yee, N., Tobin, M.J., 2004. Molecular characterization of cyanobacterial silicification using synchrotron infrared micro-spectroscopy. *Geochim. Cosmochim. Acta* **68** (4), 729–741.
- Canfield, D.E., 1998. A new model for Proterozoic ocean chemistry. *Nature* **396** (6710), 450–453.
- Claessens, J., van Lith, Y., Laverman, A., Van Cappellen, P., 2006. Acid-base activity of microorganisms. *J. Geochem. Explor.* **88** (1–3), 181–185.
- Conley, D.J., 2002. Terrestrial ecosystems and the global biogeochemical silica cycle. *Global Biogeochem. Cycles* **16** (4).
- Coradin, T., Durupthy, O., Livage, J., 2002. Interactions of amino-containing peptides with sodium silicate and colloidal silica: a biomimetic approach of silicification. *Langmuir* **18** (6), 2331–2336.
- Coradin, T., Lopez, P.J., 2003. Biogenic silica patterning: simple chemistry or subtle biology? *ChemBiochem* **4** (4), 251–259.
- Daye, S., Champmartin, D., Rubini, P., Berthon, G., 2002. Aluminium speciation studies in biological fluids. Part 8. A quantitative investigation of Al(III)-amino acid complex equilibria and assessment of their potential implications for aluminium metabolism and toxicity. *Inorg. Chim. Acta* **339**, 513–524.
- de Ronde, C.E.J., Stoffers, P., Garbe-Schonberg, D., Christenson, B.W., Jones, B., Manconi, R., Browne, P.R.L., Hissmann, K., Botz, R., Davy, Schmitt, M., Battershill, C.N., 2002. Discovery of active hydrothermal venting in Lake Taupo, New Zealand. *J. Volcanol. Geother. Res.* **115** (3–4), 257–275.
- Decho, A.W., Kawaguchi, T., 1999. Confocal imaging of in situ natural microbial communities and their extracellular polymeric secretions using Nanoplast (R) resin. *Biotechniques* **27** (6), 1246–1252.
- Dietzel, M., 2000. Dissolution of silicates and the stability of polysilicic acid. *Geochim. Cosmochim. Acta* **64** (19), 3275–3281.
- Dietzel, M., Usdowski, E., 1995. Depolymerization of soluble silicate in dilute aqueous-solutions. *Colloid Polym. Sci.* **273** (6), 590–597.
- Djordjevic, P., Jelic, R., 1997. Solution equilibria in L-glutamic acid and L-serine plus iron(III) systems. *Trans. Met. Chem.* **22** (3), 284–293.
- Dong, H.L., Kostka, J.E., Kim, J., 2003. Microscopic evidence for microbial dissolution of smectite. *Clay Clay Miner.* **51** (5), 502–512.
- Fein, J.B., Scott, S., Rivera, N., 2002. The effect of Fe on Si adsorption by *Bacillus subtilis* cell walls: insights into non-metabolic bacterial precipitation of silicate minerals. *Chem. Geol.* **182** (2–4), 265–273.
- Follmi, K.B., 1996. The phosphorus cycle, phosphogenesis and marine phosphate-rich deposits. *Earth Sci. Rev.* **40** (1–2), 55–124.
- Fortin, D., Beveridge, T.J., 1997. Role of the bacterium *Thiobacillus* in the formation of silicates in acidic mine tailings. *Chem. Geol.* **141** (3–4), 235–250.
- Fortin, D., Ferris, F.G., 1998. Precipitation of iron, silica, and sulfate on bacterial cell surfaces. *Geomicrobiol. J.* **15** (4), 309–324.
- Francis, S., Margulis, L., Barghoorn, E.S., 1978. Experimental Silicification of Microorganisms. 2. Time of Appearance of Eukaryotic Organisms in Fossil Record. *Precambrian Res.* **6** (1), 65–100.
- Gates, W.P., Slade, P.G., Manceau, A., Lanson, B., 2002. Site occupancies by iron in nontronites. *Clay Clay Miner.* **50** (2), 223–239.
- Ghosal, D., Omelchenko, M.V., Gaidamakova, E.K., Matrosova, V.Y., Vasilenko, A., Venkateswaran, A., Zhai, M., Kostandarithes, H.M., Brim, H., Makarova, K.S., Wackett, L.P., Fredrickson, J.K., Daly, M.J., 2005. How radiation kills cells: survival of *Deinococcus radiodurans* and *Shewanella oneidensis* under oxidative stress. *Fems Microbiol. Rev.* **29** (2), 361–375.
- Goldhaber, M.B., Aller, R.C., Cochran, J.K., Rosenfeld, J.K., Martens, C.S., Berner, R.A., 1977. Sulfate reduction, diffusion, and bioturbation in long-island sound sediments—report of foam group. *Am. J. Sci.* **277** (3), 193–237.
- Haas, J.R., DiChristina, T.J., 2002. Effects of Fe(III) chemical speciation on dissimilatory Fe(III) reduction by *Shewanella putrefaciens*. *Environ. Sci. Technol.* **36** (3), 373–380.
- Heissenberger, A., Leppard, G.G., Herndl, G.J., 1996. Ultrastructure of marine snow. 2. Microbiological considerations. *Mar. Ecol. Prog. Ser.* **135** (1–3), 299–308.
- Heldal, M., Scanlan, D.J., Norland, S., Thingstad, F., Mann, N.H., 2003. Elemental composition of single cells of various strains of marine *Prochlorococcus* and *Synechococcus* using X-ray microanalysis. *Limnol. Oceanogr.* **48** (5), 1732–1743.
- Hovey, J.K., Tremaine, P.R., 1985. Thermodynamics of the complexes of aqueous iron(III), aluminum, and several divalent-cations with edta—heat-capacities, volumes, and variations in stability with temperature. *J. Phys. Chem.* **89** (25), 5541–5549.
- Iler, R.K., 1979. *The Chemistry of Silica*. Wiley.
- Jahnke, R.A., Emerson, S.R., Roe, K.K., Burnett, W.C., 1983. The present-day formation of apatite in mexican continental-margin sediments. *Geochim. Cosmochim. Acta* **47** (2), 259–266.
- Jiang, W., Saxena, A., Song, B., Ward, B.B., Beveridge, T.J., Myneni, S.C.B., 2004. Elucidation of functional groups on gram-positive and gram-negative bacterial surfaces using infrared spectroscopy. *Langmuir* **20** (26), 11433–11442.
- Jones, B., Renaut, R.W., Rosen, M.R., 1997. Biogenicity of silica precipitation around geysers and hot-spring vents, North Island, New Zealand. *J. Sediment. Res.* **67** (1), 88–104.
- Kasting, J.F., 1991. Box models for the evolution of atmospheric oxygen—an update. *Global Planet. Change* **97** (1–2), 125–131.
- Kawaguchi, T., Decho, A.W., 2002. In situ microspatial imaging using two-photon and confocal laser scanning microscopy of bacteria and

- extracellular polymeric secretions (EPS) within marine stromatolites. *Mar. Biotechnol.* **4** (2), 127–131.
- Kawano, M., Tomita, K., 2001. Microbial biomineralization in weathered volcanic ash deposit and formation of biogenic minerals by experimental incubation. *Am. Mineral.* **86** (4), 400–410.
- Kawano, M., Tomita, K., 2002. Microbiotic formation of silicate minerals in the weathering environment of a pyroclastic deposit. *Clay Clay Miner.* **50** (1), 99–110.
- Keeling, J.L., Raven, M.D., Gates, W.P., 2000. Geology and characterization of two hydrothermal nontronites from weathered metamorphic rocks at the Uley Graphite Mine, South Australia. *Clay Clay Miner.* **48** (5), 537–548.
- Knecht, M.R., Wright, D.W., 2004. Amine-terminated dendrimers as biomimetic templates for silica nanosphere formation. *Langmuir* **20** (11), 4728–4732.
- Konhauser, K.O., Ferris, F.G., 1996. Diversity of iron and silica precipitation by microbial mats hydrothermal waters, Iceland: implications for precambrian iron formations. *Geology* **24** (4), 323–326.
- Konhauser, K.O., Jones, B., Phoenix, V.R., Ferris, F.G., Renaut, R.W., 2004. The microbial role in hot spring silicification. *Ambio* **33** (8), 552–558.
- Konhauser, K.O., Schiffman, P., Fisher, Q.J. 2002. Microbial mediation of authigenic clays during hydrothermal alteration of basaltic tephra, Kilauea Volcano. *Geochim. Geophys. Geosys.* **3**.
- Kostka, J.E., Haefele, E., Viehweger, R., Stucki, J.W., 1999a. Respiration and dissolution of iron(III) containing clay minerals by bacteria. *Environ. Sci. Technol.* **33** (18), 3127–3133.
- Kostka, J.E., Nealson, K.H., 1998. Isolation, cultivation, and characterization of iron- and manganese-reducing bacteria. In: Burlage, R.S. (Ed.), *Techniques in Microbial Ecology*. Oxford University Press, pp. 58–78.
- Kostka, J.E., Stucki, J.W., Nealson, K.H., Wu, J., 1996. Reduction of structural Fe(III) in smectite by a pure culture of *Shewanella putrefaciens* strain MR-1. *Clay Clay Miner.* **44** (4), 522–529.
- Kostka, J.E., Wu, J., Nealson, K.H., Stucki, J.W., 1999b. The impact of structural Fe(III) reduction by bacteria on the surface chemistry of smectite clay minerals. *Geochim. Cosmochim. Acta* **63** (22), 3705–3713.
- Kroger, N., Deutzmann, R., Bergsdorf, C., Sumper, M., 2000. Species-specific polyamines from diatoms control silica morphology. *Proc. Natl. Acad. Sci. USA* **97** (26), 14133–14138.
- Kroger, N., Deutzmann, R., Sumper, M., 1999. Polycationic peptides from diatom biosilica that direct silica nanosphere formation. *Science* **286** (5442), 1129–1132.
- Leaphart, A.B., Thompson, D.K., Huang, K., Alm, E., Wan, X.F., Arkin, A., Brown, S.D., Wu, L.Y., Yan, T.F., Liu, X.D., Wickham, G.S., Zhou, J.Z., 2006. Transcriptome profiling of *Shewanella oneidensis* gene expression following exposure to acidic and alkaline pH. *J. Bacteriol.* **188** (4), 1633–1642.
- Leppard, G.G., Heissenberger, A., Herndl, G.J., 1996. Ultrastructure of marine snow. 1. Transmission electron microscopy methodology. *Mar. Ecol. Prog. Ser.* **135** (1–3), 289–298.
- Lopez-Caballero, M.E., Sanchez-Fernandez, J.A., Moral, A., 2001. Growth and metabolic activity of *Shewanella putrefaciens* maintained under different CO₂ and O₂ concentrations. *Int. J. Food Microbiol.* **64** (3), 277–287.
- Lu, C.D., 2006. Pathways and regulation of bacterial arginine metabolism and perspectives for obtaining arginine overproducing strains. *Appl. Microbiol. Biotechnol.* **70** (3), 261–272.
- Mera, M.U., Beveridge, T.J., 1993. Mechanism of silicate binding to the bacterial-cell wall in *Bacillus-Subtilis*. *J. Bacteriol.* **175** (7), 1936–1945.
- Michalopoulos, P., Aller, R.C., 2004. Early diagenesis of biogenic silica in the Amazon delta: Alteration, authigenic clay formation, and storage. *Geochim. Cosmochim. Acta* **68** (5), 1061–1085.
- Mizutani, T., Nagase, H., Fujiwara, N., Ogoshi, H., 1998. Silicic acid polymerization catalyzed by amines and polyamines. *Bull. Chem. Soc. Jpn.* **71** (8), 2017–2022.
- Mondi, C., Leifer, K., Mavrocordatos, D., Perret, D., 2002. Analytical electron microscopy as a tool for accessing colloid formation process in natural waters. *J. Microsc. Oxford* **207**, 180–190.
- Moore, P.A., Reddy, K.R., 1994. Role of Eh and Ph on phosphorus geochemistry in sediments of lake Okeechobee, Florida. *J. Environ. Qual.* **23** (5), 955–964.
- Myers, C.R., Nealson, K.H., 1988. Bacterial manganese reduction and growth with manganese oxide as the sole electron acceptor. *Science* **240**, 1319–1321.
- Norland, S., Fagerbakke, K.M., Heldal, M., 1995. Light-element analysis of individual bacteria by X-ray-microanalysis. *Appl. Environ. Microbiol.* **61** (4), 1357–1362.
- Ohmoto, H., Kakegawa, T., Lowe, D.R., 1993. 3.4-Billion-year-old biogenic pyrites from Barberton, South-Africa—sulfur isotope evidence. *Science* **262** (5133), 555–557.
- O'Reilly, S.E., Furukawa, Y., Newell, S. 2006. Dissolution and microbial Fe(III) reduction of nontronite (NAU-1). *Chem. Geol.* in press, doi:10.1016/j.chemgeo.2006.05.010.
- O'Reilly, S.E., Watkins, J., Furukawa, Y., 2005. Secondary mineral formation associated with respiration of nontronite, NAU-1 by iron reducing bacteria. *Geochem. Trans.* **6** (4), 67–76.
- Parkhurst, D.L., Appelo, C.A.J. 1999. User's guide to PHREEQC (Version 2)—A computer program for speciation, batch-reaction, one-dimensional transport, and inverse geochemical calculations. US Geological Survey Water-Resources Investigations Report.
- Perret, D., Leppard, G.G., Muller, M., Belzile, N., Devitre, R., Buffle, J., 1991. Electron-microscopy of aquatic colloids—non-perturbing preparation of specimens in the field. *Water Res.* **25** (11), 1333–1343.
- Phoenix, V.R., Konhauser, K.O., Ferris, F.G., 2003. Experimental study of iron and silica immobilization by bacteria in mixed Fe–Si systems: implications for microbial silicification in hot springs. *Can. J. Earth Sci.* **40** (11), 1669–1678.
- Portanova, R., Lajunen, L.H.J., Tolazzi, M., Piispanen, J., 2003. Critical evaluation of stability constants for alpha-hydroxycarboxylic acid complexes with protons and metal ions and the accompanying enthalpy changes part II. Aliphatic 2-hydroxycarboxylic acids. *Pure Appl. Chem.* **75** (4), 495–540.
- Poulsen, N., Sumper, M., Kroger, N., 2003. Biosilica formation in diatoms: characterization of native silaffin-2 and its role in silica morphogenesis. *Proc. Natl. Acad. Sci. USA* **100** (21), 12075–12080.
- Ragueneau, O., Treguer, P., Leynaert, A., Anderson, R.F., Brzezinski, M.A., DeMaster, D.J., Dugdale, R.C., Dymond, J., Fischer, G., Francois, R., Heinze, C., Maier-Reimer, E., Martin-Jezequel, V., Nelson, D.M., Queguiner, B., 2000. A review of the Si cycle in the modern ocean: recent progress and missing gaps in the application of biogenic opal as a paleoproductivity proxy. *Global Planet. Change* **26** (4), 317–365.
- Sarazin, G., Michard, G., Prevot, F., 1999. A rapid and accurate spectroscopic method for alkalinity measurements in sea water samples. *Water Res.* **33** (1), 290–294.
- Sjoberg, S., 1996. Silica in aqueous environments. *J. Non Crystalline Solids* **196**, 51–57.
- Skeidsvoll, J., Ueland, P.M., 1995. Analysis of double-stranded DNA by capillary electrophoresis with laser-induced fluorescence detection using the monomeric dye SYBR-Green-I. *Anal. Biochem.* **231** (2), 359–365.
- Spencer, C.P., 1983. Marine biogeochemistry of silicon. In: Aston, S.R. (Ed.), *Silicon Geochemistry and Biogeochemistry*. Academic Press, pp. 101–142.
- Sumper, M., 2004. Biomimetic patterning of silica by long-chain polyamines. *Angew. Chem. Int. Ed.* **43** (17), 2251–2254.
- Sumper, M., Brunner, E., 2006. Learning from diatoms: nature's tools for the production of nanostructured silica. *Adv. Funct. Mater.* **16** (1), 17–26.
- Sundby, B., Gobeil, C., Silverberg, N., Mucci, A., 1992. The Phosphorus Cycle in Coastal Marine-Sediments. *Limnol. Oceanogr.* **37** (6), 1129–1145.
- Swartz, C.H., Ulery, A.L., Gschwend, P.M., 1997. An AEM–TEM study of nanometer-scale mineral associations in an aquifer sand: implications for colloid mobilization. *Geochim. Cosmochim. Acta* **61** (4), 707–718.

- Tabor, C.W., Tabor, H., 1985. Polyamines in microorganisms. *Microbiol. Rev.* **49** (1), 81–99.
- Taunton, A.E., Welch, S.A., Banfield, J.F., 2000. Microbial controls on phosphate and lanthanide distributions during granite weathering and soil formation. *Chem. Geol.* **169** (3–4), 371–382.
- Toporski, J.K.W., Steele, A., Westall, F., Thomas-Keppta, K.L., McKay, D.S., 2002. Winner of the 2001 Gerald A. Soffen Memorial Award—The simulated silicification of bacteria—new clues to the modes and timing of bacterial preservation and implications for the search for extraterrestrial microfossils. *Astrobiology* **2** (1), 1–26.
- Urrutia, M.M., Beveridge, T.J., 1994. Formation of fine-grained metal and silicate precipitates on a bacterial surface (*Bacillus Subtilis*). *Chem. Geol.* **116** (3–4), 261–280.
- Venkateswaran, K., Moser, D., Dollhopf, M., Lies, D., Saffarini, D., MacGregor, B., Ringelberg, D., White, D., Nishijima, M., Sano, H., Burghardt, J., Stackebrandt, E., Neelson, K., 1999. Polyphasic taxonomy of the genus *Shewanella* and description of *Shewanella oneidensis* sp. nov. *Int. J. Syst. Bacteriol.* **49** (2), 705–724.
- Vieillard, P., 2000. A new method for the prediction of Gibbs free energies of formation of hydrated clay minerals based on the electronegativity scale. *Clay Clay Miner.* **48** (4), 459–473.
- Viollier, E., Inglett, P.W., Hunter, K., Roychoudhury, A.N., Van Cappellen, P., 2000. The ferrozine method revisited: Fe(II)/Fe(III) determination in natural waters. *Appl. Geochem.* **15** (6), 785–790.
- Washington, J.W., Endale, D.M., Samarkina, L.P., Chappell, K.E., 2004. Kinetic control of oxidation state at thermodynamically buffered potentials in subsurface waters. *Geochim. Cosmochim. Acta* **68** (23), 4831–4842.
- Webb, S.M., Leppard, G.G., Gaillard, J.F., 2000. Zinc speciation in a contaminated aquatic environment: characterization of environmental particles by analytical electron microscopy. *Environ. Sci. Technol.* **34** (10), 1926–1933.
- Westall, F., Boni, L., Guerzoni, E., 1995. The experimental silicification of microorganisms. *Palaeontology* **38**, 495–528.
- Wilkinson, K.J., Balnois, E., Leppard, G.G., Buffle, J., 1999. Characteristic features of the major components of freshwater colloidal organic matter revealed by transmission electron and atomic force microscopy. *Colloids Surf. a-Physicochem. Eng. Aspects* **155** (2–3), 287–310.
- Yee, N., Phoenix, V.R., Konhauser, K.O., Benning, L.G., Ferris, F.G., 2003. The effect of cyanobacteria on silica precipitation at neutral pH: implications for bacterial silicification in geothermal hot springs. *Chem. Geol.* **199** (1–2), 83–90.